Journal of Materials Chemistry

Dynamic Article Links

Cite this: J. Mater. Chem., 2012, 22, 19488

www.rsc.org/materials

PAPER

Dendritic polyglycerolamine as a functional antifouling coating of gold surfaces†‡

Julieta I. Paez,[a] Verónica Brunetti,[b] Miriam C. Strumia,[a] Tobias Becherer,[c] Tihomir Solomun,§[d] Jorge Miguel,¶[e] Christian F. Hermanns,[e] Marcelo Calderón[c] and Rainer Haag*[c]

Received 20th April 2012, Accepted 28th May 2012
DOI: 10.1039/c2jm32486e

Dendritic polyglycerol (PG) functionalized surfaces represent a good alternative for preparation of protein resistant materials, whose versatility can be enhanced by conferring them the ability to bind particular biomolecules of interest to the surface. In this work, PG derivatives bearing disulfide and different loadings of amino moieties (0–14%) were synthesized and attached to gold surfaces. The modified surfaces were characterized by means of infrared reflection adsorption spectroscopy (FT-IRRAS), X-ray photoelectron spectroscopy (XPS), and contact angle measurements. The protein resistance properties of the PG-modified surfaces were evaluated by surface plasmon resonance (SPR) spectroscopy using fibrinogen, albumin, pepsin, and lysozyme as model proteins. The availability and accessibility of the amino groups to bind biomolecules were assessed by fluorescence measurements. This study demonstrates that PG-coated surfaces with amino contents up to 9% still show very good protein resistant properties. At the same time, the amino moieties on the surface are available and reactive for selective ligand attachment. By fluorescence labeled DNA hybridization, the high selectivity of these functional surfaces could be demonstrated.

Introduction

The study and development of resistant, antibiofouling surfaces have proved to be of significant value in biotechnology, biomedicine, bioelectronics, health care, energy, food, and marine industries.[1–5] Particularly, materials capable of resisting non-specific protein adsorption are of great importance in biomaterials and biomedical applications, including implants, biosensors, and nanocarriers for drug delivery.[3,5,6] Indeed, the ability to resist non-specific protein adsorption is a major indicator of a material's biological inertness or biocompatibility.[6] Non-specific protein adsorption is a process that occurs when a solid substrate is immersed in biological fluids, and comprises the physical adsorption of circulating proteins on the material surface without specific receptor-recognition interactions.[3] Furthermore, non-specific adsorption initiates the foreign body reaction causing a walling off of the implanted device which may lead to the improper function of the device.[7] Therefore, tailoring the materials surface chemistry using synthetic strategies is crucial for producing surfaces with defined (bio)specific bindings as well as repellant properties.

A well-established strategy in the design of resistant devices is coating the surface with a layer of a material that reduces non-specific protein interactions, which may be introduced for example in the form of self-assembled monolayers (SAMs)[3,8] or polymer brushes.[3,9] A wide range of resistant coatings have been reported so far, and based on the analysis of the best protein resistant surfaces known in the literature,[8,10–13] it seems that desirable features for resistant coatings are: (a) highly flexible aliphatic polyether architecture, (b) hydrophilic, hydrogen-bondable groups, and (c) overall electrical neutrality. Poly(ethylene glycols) (PEGs) are the most commonly used resistant benchmark materials. PEGs are highly hydrophilic, linear, flexible, water-soluble polyethers, which are relatively non-immunogenic, non-toxic at low doses, and with proven antifouling

[a]*IMBIV-CONICET, Departamento de Química Orgánica, Facultad de Ciencias Químicas, Universidad Nacional de Córdoba, Haya de la Torre y Medina Allende, Ciudad Universitaria, X5000HUA Córdoba, Argentina*
[b]*INFIQC-CONICET, Departamento de Fisicoquímica, Facultad de Ciencias Químicas, Universidad Nacional de Córdoba, Haya de la Torre y Medina Allende, Ciudad Universitaria, X5000HUA Córdoba, Argentina*
[c]*Institut für Chemie und Biochemie, Organische und Makromolekulare Chemie, Freie Universität Berlin, Takustrasse. 3, 14195 Berlin, Germany. E-mail: haag@chemie.fu-berlin.de; Fax: +49 30 838 53357; Tel: +49 30 838 52633*
[d]*Institut für Chemie und Biochemie, Physikalische und Theoretische Chemie, Freie Universität Berlin, Takustrasse. 3, 14195 Berlin, Germany*
[e]*Institut für Experimentalphysik, Freie Universität Berlin, Arnimallee 14, 14195 Berlin, Germany*

† This article is submitted to the themed issue Materials for Biosurfaces, guest-edited by Christopher K. Ober.

‡ Electronic supplementary information (ESI) available: Synthesis and spectroscopic characterization of PG derivatives, and supporting figures. See DOI: 10.1039/c2jm32486e

§ Present address: Federal Institute for Materials Research and Testing, Division 6.9, Nanotribology and Nanostructuring of Surfaces. Unter den Eichen 87, 12205, Berlin, Germany.

¶ Present address: Diamond Light Source, Harwell Science & Innovation Campus, OX11 0DE Chilton, Didcot, UK.

properties.[14,15] Despite their wide use, PEGs present some drawbacks like stability issues, since they can be oxidized in a physiological environment spontaneously or enzymatically.[14,16] Moreover, PEG offers just a low binding capacity due to the presence of functional groups only at the chain ends. Thus, the investigation of novel routes to prepare antifouling matrices is a subject of active research.

Dendritic polyglycerols (PGs) are aliphatic polyols that combine a stable, biocompatible polyether scaffold, high-end group that allows for further functionalization and a compact, well-defined dendrimer-like architecture.[6] These polymers exhibit good chemical/thermal stability and inertness under biological conditions and are highly biocompatible, characteristics that can be exploited to generate new material properties for many pharmaceutical and biomedical applications. Their multifunctional macromolecular scaffold is expected to lead to new strategies for nanomedicine[17] as well as for regenerative medicine in the form of non-fouling surfaces.[6] Thus, PGs constitute a good alternative to PEG as a coating material for surface modification to obtain biocompatible and functional materials.

In 2004, monolayers based on dendritic PG were shown to render gold surfaces highly protein resistant. In this study, different PG derivatives bearing hydroxy- or methoxy-end groups were covalently immobilized on gold surfaces and investigated with respect to the adsorption of single proteins.[18] The PG-coated surfaces were as protein resistant as PEG SAMs and significantly better than a carboxymethyldextran surface (commercially available CM5 chip from Biacore),[19] whereas the bulk PG also showed a higher thermal stability than PEG. Partially methylated PG derivatives did not reveal significantly different protein resistance to the best hydrophilic hydroxyl-PG derivative. This study clearly demonstrates that hydrophilic PGs with a high number of –OH groups are yet another exception to the correlation between protein resistance and the absence of H-bond donors,[8,10] in a similar way to mannitol SAMs[12] and dextran-coated surfaces.[13] Additionally, the highly branched architecture with a number of functional groups allows further postsynthetic modification and multivalent functionalization.

After this pioneer study, the Kizhakkedathu group[20] reported the preparation of PG-coated surfaces and demonstrated that branched polymers produced more uniform structures on gold with low surface roughness. In another study by Wang *et al.*[21] PGs were grown from the surface of magnetic nanoparticles, and the nanocomposites showed excellent protein resistance properties, similar to PEGylated nanoparticles.

To gain a deeper insight into the underlying mechanism of protein resistance, our group recently prepared a large variety of PG derivatives to assess their protein-repellant capability.[22,23] In a first approach, a library of mono-amino oligoglycerols with terminal –OH or $–OCH_3$ functionality was synthesized and coupled to gold surfaces through the "anhydride" method.[22] Surface plasmon resonance (SPR) spectroscopy revealed that the capability of PG dendrons to resist non-specific protein adsorption strongly depends on the coating density, surface functionality, size, degree of branching, and structural freedom (*i.e.*, disorder and flexibility/chain mobility) of the PG structures. Furthermore, methylation of hyperbranched PG also improved the protein resistance. In a second approach, a family of PG dendrons that had an alkanethiolate group at the focal point and different terminal functionalities (–OH, $–OCH_3$) was synthesized and then attached to gold surfaces by a direct chemisorption. We observed that even relatively small oligomers can be protein resistant. More recently, we studied the dependence of polymer brush architecture on protein resistance by preparing novel polymer brushes with different side chains based on oligoglycerols,[24] as well as the application of PG in the construction of bioinert glass.[25]

On the basis of these findings, it becomes clear that PG-coated surfaces represent a good alternative towards the preparation of resistant materials, whose versatility can be enhanced by conferring them the ability to bind particular biomolecules of interest to the surface. The combination of both characteristics has been demonstrated to be crucial, for example, in the fabrication of biosensing platforms for analyses in biological samples.[3,26,27] This goal might be achieved by introducing amino moieties in the PG scaffold. Despite the fact that amino groups can be used as anchoring sites, their presence also causes a negative effect on the protein resistant properties of the surface. This effect has been associated with two aspects, the inclusion of hydrogen-bond donors[8,11] and the presence of a net charge under physiological conditions. Non-specific protein adsorption is known to be exacerbated on cationic surfaces relative to neutral surfaces.[8] Previous studies carried out on SAMs,[28] mixed SAMs,[29] and several polymeric coatings[11] presenting amino groups have assessed this effect. However, to the best of our knowledge, no systematic studies addressing this issue in dendritic polymers have been reported so far.

Therefore, herein we report on the synthesis of a family of dendritic PGs that have disulfide anchor groups and different amino contents and their use to coat gold substrates by self-assembly. The successful attachment of PG was monitored by means of infrared reflection adsorption spectroscopy (FT-IR-RAS), X-ray photoelectron spectroscopy (XPS), and contact angle measurements. The protein resistance properties of the PG-modified surfaces were assessed through SPR, using fibrinogen, albumin, pepsin, and lysozyme as model proteins. The main focus of this work is evaluating the effect of the amino content on the protein resistance of these dendritic polymers, in order to determine (a) the maximum number of amino moieties that can be introduced to still observe an excellent protein resistance and (b) whether the amino groups remain available and accessible enough to act as useful attachment points for linking biomolecules, as a model of bioactive surfaces.

Experimental part

General

^{1}H NMR and ^{13}C NMR spectra were recorded on ECX 400 (400 MHz for ^{1}H) as well as on Delta JEOL Eclipse 500 (500 MHz for ^{1}H) spectrometers at 25 °C in methanol-d_4 (Deutero GmbH, Germany). The spectra were calibrated using the solvent residual peak. Transmission IR spectra (KBr) were recorded on a Nicolet 5SXC FTIR spectrometer.

Materials

The starting polyglycerol, PG–OH, was synthesized according to the literature[30] and had the following characteristics: average

M_n = 5000 g mol^{-1}, trimethylolpropane (TMP) core, *ca.* 13.5 mmol –OH g^{-1} polymer. Unless stated otherwise, the following reagents and solvents were purchased from Acros Organic, Aldrich, or Fluka, and used as received: methanesulfonyl chloride (MsCl), sodium azide (NaN_3), triphenylphosphine (PPh_3), 6,8-dithiooctanoic acid (DL-thioctic acid, TA), *N*,*N*′-dicyclohexylcarbodiimide (DCC), *N*,*N*′-dimethylaminopyridine (DMAP), hydrogen peroxide, sulfuric acid, hexadecanethiol (HDT), and sodium dodecylsulfate (SDS). Dry and analytical grade solvents: pyridine, methanol, and *N*,*N*-dimethylformamide, were purchased from Acros or Aldrich and used as received. The bifunctional crosslinker sulfosuccinimidyl 4-(*N*-maleimidomethyl)cyclohexane-1-carboxylate (sulfo-SMCC, No-Weigh format) was purchased from Thermo Scientific and stored at −20 °C until use. HPLC purified oligonucleotides with the structure 5′-HS-$(CH_2)_6$-$(dT)_{25}$-3′ and its dye-labeled complementary strand $(dA)_{25}$-Cy5 used for hybridization (henceforth referred to as HS-dT25 and dA25-Cy5, respectively) were obtained from Thermo Electron. Fluorescent-labeled streptavidin, Strept-Cy3 from *Streptomyces avidinii*, was acquired from Sigma. Fibrinogen (Fib, from bovine plasma, F8630), lysozyme (Lys, chicken egg white, E.C. 3.2.1.17, L6876), pepsin (Pep, porcine gastric mucosa, E.C. 3.4.23.1, P7012) and albumin (Alb, bovine serum albumin, Cohn Fraction V, A7030) were purchased from Sigma-Aldrich (Steinheim, Germany) and used without further purification. Phosphate buffered saline (PBS; 1×, pH 7.4) was purchased from BioWhittaker. PBS solutions were freshly prepared by dilution in deionized water and degassed by filtration through 0.22 μm filters prior to use. Protein solutions (1 mg mL^{-1} in PBS) and SDS solutions (1 wt% and 4 wt% in PBS) were freshly prepared, filtered through 0.22 μm syringe filters and degassed in an ultrasound bath at room temperature. Water was purified using a Millipore Milli-Q system. All solutions were prepared immediately prior to their use. Reactions requiring dry conditions were carried out in dried Schlenk glassware under argon. Dialysis was performed in benzoylated cellulose dialysis tubes from Sigma-Aldrich (diameter 32 mm, molecular weight cut-off (MWCO) 1000 g mol^{-1}). Piranha solution was prepared from 3 : 1, v/v, H_2SO_4–H_2O_2 and used immediately. Piranha solution reacts violently with organic materials and should be handled with extreme care. IRRAS, XPS, confocal fluorescence microscopy and contact angle measurements were conducted over 12 × 12 × 0.7 mm gold substrates on borosilicate glass (Arrandee, Germany). XPS studies were performed over gold-coated mica wafers (Georg Albert Physical Vapor Deposition, Germany). SPR studies were measured using gold chips (SIA Kit Au) purchased from Biacore (Uppsala, Sweden) and stored at 4 °C.

Synthesis of polyglycerol derivatives

The synthesis of PG derivatives was carried out following procedures reported in the literature[18,31] (see ESI‡). Varying the experimental conditions and adjusting the solubility of the products were necessary to prepare PG compounds with a controlled loading of amino and disulfide groups.

Precleaning of bare gold surfaces and their functionalization by self-assembly

Gold surfaces were precleaned prior to use by immersing the substrates into fresh piranha solution for 1 min, rinsing copiously with water for 1 min, then rinsing with EtOH for 1 min, and finally drying under a stream of N_2. The surface was functionalized by immersing the substrate overnight into a 1 mM solution of the corresponding PG derivative in MeOH. The modified gold surface was removed and rinsed copiously with MeOH for 1 min, and then with EtOH for another minute before drying with N_2. The functionalized surface was used immediately.

Characterization of the modified gold surfaces

FT-IRRAS. The spectra were recorded with a Nicolet 8700 (Thermo Electron) spectrometer equipped with the external reflection accessory (85° grazing angle) and a MCT detector cooled with liquid nitrogen. The measurement chamber and instrument were continuously purged with dry N_2. The latter was previously purified through molecular sieves and a PEFT membrane made by active carbon. Spectra were taken as the average of 2048 scans at a 4 cm^{-1} resolution. A precleaned bare gold surface was used as reference. All spectra were expressed in extinction units after linear baseline corrections.

XPS studies. XPS measurements were realized by means of a SPECS Phoibos 100 electron analyzer at a typical energy resolution of 600 meV at 20 eV pass energy. An Mg Kα X-ray tube was used as the light source, with excitation photon energy of 1253.6 eV, resulting in energy resolutions of 800 meV. The electron take-off angle was set to 0°, corresponding to normal emission. The binding energies have been calibrated to the Au $4f_{7/2}$ peak at 84.0 eV. Components in the XPS spectra were fitted using linear and Shirley line profiles for the backgrounds and a product of Gaussian and Lorentzian functions for the C 1s, O 1s and N 1s peaks. The S 2p XPS spectra were fitted using two doublets corresponding to the S $2p_{3/2}$ and S $2p_{1/2}$ signals. For each doublet, the two peaks had a 1.2 eV energy splitting and an area ratio of 2 : 1. The base pressure in the analysis chamber during the measurements was better than 1 × 10^{-9} mbar.

Contact angle measurements. The water contact angles on the modified gold surfaces were measured with a Ramé-Hart model 1000 contact angle goniometer under ambient conditions. Water drops (2 μL) were delivered to the surface using a micrometer syringe (Gilmont). The reported values of the contact angles were the average of three to five measurements taken at different locations on the surface. The values of all replicates were within ±3° of the mean. Precleaned bare gold chips were used as reference.

Confocal fluorescence microscopy. Confocal fluorescence images were obtained with an Affimetrix 418 microarray scanner and analyzed with GenePixPro 6.0 software, after subtracting the local background. Fluorescent probes were attached to the PG-modified chips by two different paths, specific DNA coupling, and a non-specific streptavidin attachment, as follows:

Non-specific streptavidin attachment. Strept-Cy3 drops (1 mg mL^{-1} solution in 0.01 M PBS buffer, pH 7.4) were placed on a PG-modified surface as separate spots (0.5 μL each, *ca.* 1 mm diameter) using a micropipette and allowed to react for 4 h. The chip was washed with buffer to remove excess protein (5 min under shaking), immersed briefly in water, dried with N_2, and measured immediately.

Specific DNA coupling. The PG-functionalized surface was immersed in a 1 mg mL^{-1} sulfo-SMCC solution (in 0.1 M PBS buffer, 0.2 M NaCl, pH 7.4) for 2 h. After washing to remove excess crosslinker, HS-dT25 in PBS buffer was deposited onto the surface as separate spots (0.5 μL drops, about 1 mm diameter) using micropipette and allowed to react for 2 h. The chip was washed with buffer, the attached strand was hybridized with its labeled complementary strand dA25-Cy5 and the surface was washed again and measured immediately.

SPR studies

The adsorption of the test proteins to the PG-modified surfaces was carried out according to a protocol previously reported by Whitesides,[32] on a Biacore 3000 Instrument (Biacore, Uppsala, Sweden) on four independent flow cells. Briefly, the measuring protocol is as follows: (a) passing SDS (1 wt% in PBS) over the functionalized surface for 3 min and then rinsing the surface with PBS buffer for 10 min; (b) passing the adequate single-protein solution (1 mg mL^{-1} in PBS) for 25 min and then allowing PBS buffer to flow over the surface for 10 min; and finally (c) passing SDS (4 wt% in PBS) for 10 min, followed by PBS buffer for additional 10 min. The flow rate used for all experiments was 10 μL min^{-1}. The response signal from the measurement is given in response units (RU). The baseline difference given in response units (ΔRU_{sample}) before and after exposure of the sample surface to a protein solution was evaluated relative to the baseline difference (ΔRU_{HDT}) of a hydrophobic HDT reference surface according to the equation given below in percentage of protein adsorption (%PA). The adsorbed amount of proteins on HDT is assumed to be a monolayer of proteins and therefore the resulting difference in response units was set to 100% protein adsorption.[8]

$$PA\ [\%] = (\Delta RU_{sample}/\Delta RU_{HDT}) \times 100\%.$$

Results and discussion

Experimental design and synthetic approach

The fabrication of polymer-modified surfaces *via* a grafting-to approach is a simple and common procedure. Since architectural parameters, such as molecular weight distribution, branching, and functionalities can be tuned during the synthesis of the polymeric adsorbates previous to their surface attachment, films with well-defined properties and functions can be prepared.[33] Particularly, dendritic PG with molecular weights in a wide range (1–10 kDa),[30] narrow polydispersity (PDI, typically within 1.2–1.7), and several functionalities can be tailored during polymerization or subsequent functionalization steps.[6,34]

In this work, different dendritic PG adsorbates with controlled loadings of amino and disulfide moieties that can be adhered to gold were first synthesized and then attached to the above-mentioned surfaces. Disulfide groups are expected to act as surface-anchorage functions that provide stable attachment of the polymeric adsorbates to the substrates; amino groups are also expected to be involved in the immobilization process.[35] It was considered important to introduce low loadings of amino groups in these PG derivatives, to avoid non-specific protein adsorption on the surfaces. The main chemical structural feature modified on the PG coatings was the increasing variation in their amino content (from 0 to 14%). This parameter changed the hydrogen-donating ability, surface net charge under physiological conditions, and gold-stickiness characteristics of these derivatives, therefore affecting several properties like surface wettability and/or the protein repellant capability of the surfaces.

Synthesis of PG derivatives

In order to prepare PG derivatives with a controlled loading of amino and disulfide groups, a multistep synthetic strategy was used. The pathway involved mesylation, azidation, and reduction stages (Fig. 1) to convert a given number of –OH groups to $–NH_2$ groups, followed by amidation with thioctic acid (TA).

PG derivatives with 6.5, 9, and 14% amino groups were prepared with excellent yields, typically ≥90% in each step (see Table 1, entries 2–4). Throughout this paper, the notation used for the products reflects the degree of conversion of hydroxyl groups. For example, in the compound PG–OMs 9%, 9% of the –OH groups were converted into mesyl groups; in PG–NH_2 14%, 14% of hydroxyl groups were converted into amino moieties. The products were characterized spectroscopically by ^{1}H NMR and IR (Fig. S1 and S2‡), and the spectra were in agreement with those reported in the literature.[31]

Subsequently, a controlled number of disulfide groups were attached to the PG derivatives through TA coupling (Table 1, entries 6–8). The stoichiometric amount of TA was set up in order to statistically introduce one disulfide group per PG molecule. The successful preparation of the products, TA–PG–NH_2, was confirmed by NMR and IR studies (Fig. S1–S3‡). In particular, ^{1}H NMR spectroscopy showed that TA binding takes place by amidation and permitted calculation of the loading of disulfide moieties per PG molecule (N_{TA}) by comparing the spectra of the precursors and products (Fig. S3‡).

A fourth PG derivative, TA–PG–NH_2 0%, was synthesized by coupling TA directly to the starting PG through esterification (Fig. 1(v)); note that the notation used for the product reflects the absence of amino groups in this molecule, *i.e.* it has only –OH and disulfide groups. This compound will be used as a blank in the following sections.

The average number of disulfide moieties incorporated in each substrate was found to be dependent on the number of amino groups previously introduced (Table 1, entries 5–8), since TA coupling increased with the increase of the amino content in the molecule. Moreover, when TA binding took place through amidation (entries 6–8) instead of esterification (entry 5), the coupling efficiency increased and a better control over the number of bound disulfide groups could be exerted. Note that the number of disulfide moieties bound through amidation was close to one, as expected, and that the lower incorporation of TA moieties to TA–PG–NH_2 0% ($N_{TA} = 0.3$) was likely due to the

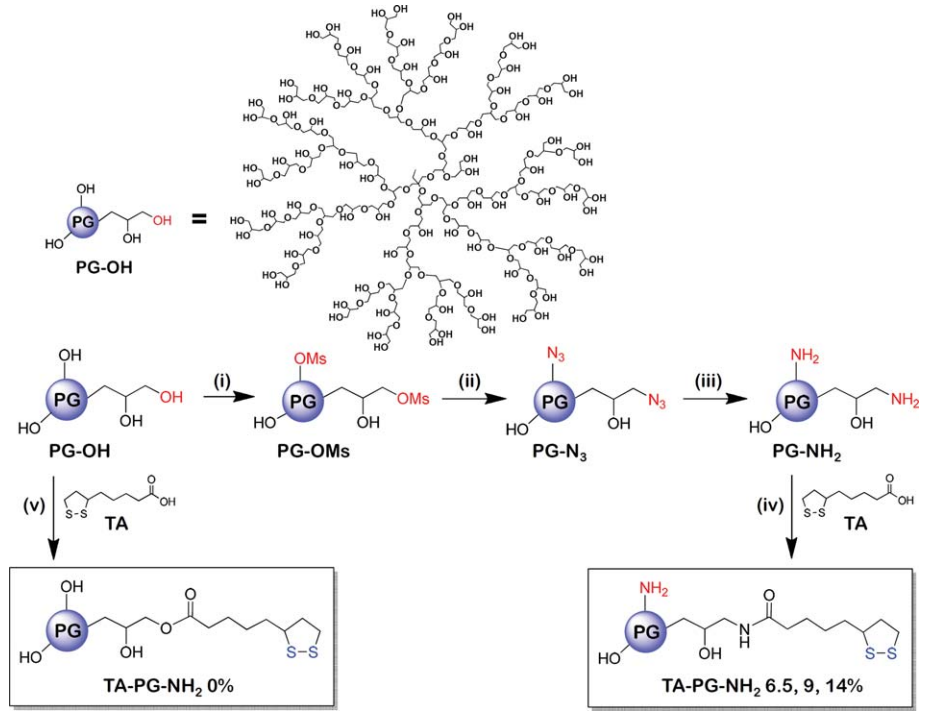

Fig. 1 Synthesis of PG derivatives through mesylation (i), azidation (ii), reduction (iii) and TA coupling (iv and v) steps. *Reagents and conditions*: (i) MsCl, dry pyridine, 0 °C–rt, 18 h, (ii) NaN_3, dry DMF, 60 °C, 72 h, (iii) PPh_3, THF–water, rt, 3 days, (iv) and (v) DCC, DMAP, DMF, 0 °C–rt, 18 h. The percentages indicate the PG amino content.

lower nucleophilicity of hydroxyl groups compared to the amino groups. These results confirm the success of the synthesis of PG derivatives with a controlled number of amino and disulfide groups, justifying the synthetic pathway used.

Preparation and characterization of PG-derivatized gold surfaces

After synthesizing the dendritic TA–PG–NH_2 derivatives, they were immobilized on gold surfaces *via* self-assembly following a dipping procedure (Fig. 2). The modified surfaces were characterized by FT-IRRAS, XPS, and contact angle studies.

FT-IRRAS studies. The coupling of PG-derivatives on gold surfaces was initially followed by means of FT-IRRAS measurements. The recorded spectra (Fig. 3) show bands located at 3500–3100 cm^{-1} (broad, O–H alcohols str.), 3000–2850 cm^{-1} (aliphatic C–H str.), and 1150–1000 cm^{-1} (broad, C–O–C ethers, secondary and primary alcohols str.),[36] which are characteristic signals of the PG scaffold and demonstrate the successful attachment of these derivatives on gold. At low amino content (6.5%, Fig. 3(b)), the spectrum is almost identical to the one for the sample without amino groups (0%, Fig. 3(a)). At higher amino contents (9 and 14%, Fig. 3(c) and (d)), the slight increment in the intensity of the bands at 1650–1550 cm^{-1} (assigned to the N–H bending of non-associated amino groups)[36] could be indicative of the presence of amino moieties on the samples. Additionally, there is a band at *ca.* 1740 cm^{-1} which grows upon increased amino content. This band could be assigned to the N–H bending of associated amino groups,[36] either due to hydrogen bonding formation or to the interaction of the amino groups with the gold surface. Other characteristic signals associated with –NH_2 groups, like N–H stretching (3500–3400 cm^{-1}) or C–N stretching (1250–1020 cm^{-1}),[36] would overlap with the O–H stretching and C–O–C stretching bands and are not clearly seen.

Table 1 Results of the PG derivatives synthesis

		Yield [%][b], X =						
Entry	Product[a]	–OMs	–N_3	–NH_2	Entry	Product of TA coupling	Yield [%]	N_{TA}[c]
1	PG–X 0%	—	—	—	5	TA–PG–NH_2 0%	95	0.3
2	PG–X 6.5%	>98	72	97	6	TA–PG–NH_2 6.5%	97	0.7
3	PG–X 9%	97	86	92	7	TA–PG–NH_2 9%	97	0.8
4	PG–X 14%	93	90	95	8	TA–PG–NH_2 14%	92	1.0

[a] X = –OMs (mesylation), –N_3 (azidation), –NH_2 (reduction). [b] Yield according to the percentage of conversion of hydroxyl groups. [c] N_{TA} = average number of TA moieties incorporated per PG molecule.

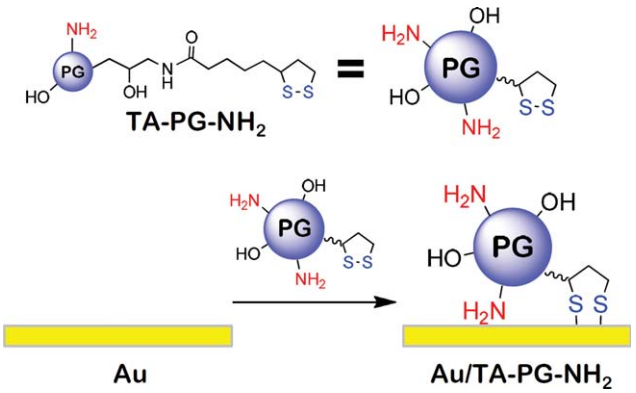

Fig. 2 Schematic representation of the self-assembly of PG derivatives on gold substrates. *Conditions*: dipping in 1 mM solution of TA–PG–NH_2 in MeOH, immersion time = 1–24 h.

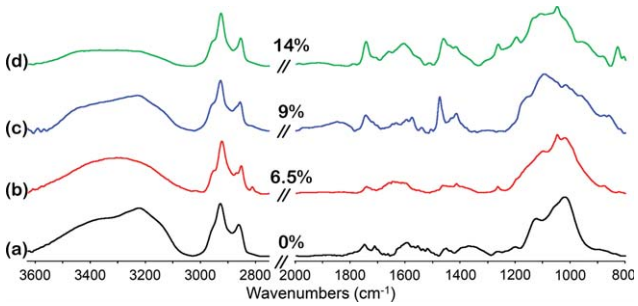

Fig. 3 Normalized FT-IRRAS spectra of Au/TA–PG–NH_2 at different amino contents: (a) 0%, (b) 6.5%, (c) 9%, and (d) 14%.

Previous studies on the self-assembly of amine-terminated PAMAM[35,37] and PEI[37] and disulfide-ended polyphenylene dendrimers[38] on gold surfaces highlighted the importance of these moieties in the adsorption process. Thus, to prove the role played by the different functional groups of PG-derivatives in their adsorption on gold, comparative studies were carried out by analyzing the self-assembly of PGs having different moieties. Both TA–PG–NH_2 0% (which lacks amino groups) and PG–NH_2 9% (which has no disulfide moieties, spectra not shown) were capable of self-assembly on gold. These results are evidence that both disulfide and amino groups play a key role in the adsorption process.

It is important to mention that prior reports demonstrated that disulfide groups form rather stable thiolate–gold bonds whereas the amine–gold interaction is much weaker,[37] which means that a number of amino groups still remained unassociated and reactive. This important point will be discussed later on in more detail.

XPS studies. As seen by FT-IRRAS measurements, the different TA–PG–NH_2 adsorbates can bind to the gold surface *via* either the disulfide or the amino group. Thus, to further explore the mechanisms of the surface attachment of the PG derivatives on gold, XPS studies were conducted. This technique offers high surface sensitivity and detailed chemical information.

C 1s, O 1s, N 1s, and S 2p XPS signals over the binding energy are plotted in Fig. 4 for the four PG-coated gold surfaces with different amino contents, after normalization to the corresponding Au $4f_{7/2}$ peak intensities subsequently taken after each region, and correcting for the atomic sensitivity factors of each species.[39] A significant increase in all four signals with the amino content is apparent, especially for the more abundant C and O species. The C 1s and O 1s spectra present maximum values for the binding energy around 286.0 eV and 532.7 eV, respectively, consistent with the etheric carbon and oxygen species present in the PG scaffold.[23]

Despite the three-dimensional character of the dendritic PG adsorbates that makes any thickness estimate a challenging task, XPS has been used to gain information about the layer thickness of SAMs of alkanethiolate chains on Au.[23] The measured C 1s to Au $4f_{7/2}$ intensity ratios and an attenuation length of 3.03 nm[40] were used to estimate the layer thicknesses using a material independent method[41] that assumes the same density for all four SAMs (see Table 2). It yields increasing apparent thickness values from 1 to 3 nm for the modified surfaces with higher amino content and with a 30% uncertainty. Taking into account that reported hyperbranched PG of MW 5 kDa have diameters between 2 and 3 nm,[6] it can be assumed that TA–PG–NH_2 form only a partially covered single layer, in good accordance with atomic force microscopy images (see Fig. S4‡).

The N 1s spectra of the amino-containing monolayers systematically present two peaks around 399.5 eV (blue dotted lines) and 400.5 eV (red dashed lines), whereas the N 1s signal for the 0% amino content shows a single peak at 399.5 eV (blue dotted line). Therefore, the low-energy peaks for which areas are rather invariant with the amino content are assigned to nitrogen species present on the surface before the PG self-assembly, probably originated during the cleansing process of the Au–mica wafers. The peak at 400.5 eV is consistent with the binding energy of NHC=O[42] and $-NH_2$,[43] and as expected, it displays a linear increase of the area with the nominal amino content of the PG derivatives.

The S 2p spectra show two doublets corresponding to two different species: gold-bound thiolate with the S $2p_{3/2}$ peak centered around 161.6 eV (red dashed lines), and unbound disulfide at 163.3 eV (ref. 44) (blue dotted lines). The S $2p_{3/2}$ intensity ratio between the two species only increases slightly

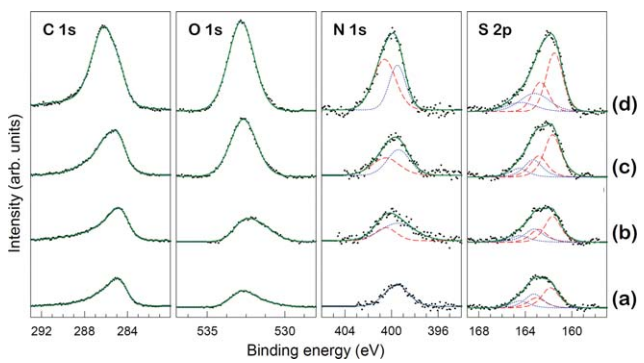

Fig. 4 XP spectra for the core-level regions of the key elements in the PG-coated surfaces with increasing amino content (a) 0%, (b) 6.5%, (c) 9%, and (d) 14%. For the N 1s and S 2p signals individual fitting peaks are shown in red dashed and blue dotted lines, whereas the fitted envelope spectra are shown in green.

Table 2 Normalized C 1s to Au $4f_{7/2}$ intensity ratio, estimated layer thickness, normalized S $2p_{3/2}$ intensities for the thiolate and disulfide species, and relative fraction of bound sulfur atoms to the gold surface in the four PG-coated gold surfaces

TA–PG–NH_2 X amino (%)	Norm. C 1s[a]	t (nm)[b]	Thiolate I_{norm}	Disulfide I_{norm}	S bound (%)
0	0.345	0.91	0.012	0.008	59.2
6.5	0.441	1.17	0.014	0.009	67.9
9	0.606	1.51	0.024	0.010	81.6
14	1.205	2.73	0.031	0.017	88.6

[a] Norm. C 1s = $(I_{C\ 1s}/S_C)/(I_{Au\ 4f}/S_{Au})$. [b] Apparent thickness values calculated assuming a constant material density.

from almost 60% to 70% with the amino percentage. However, the bound S atoms are at the bottom of the layer whereas it can be assumed that the unbound S atoms are uniformly distributed in the monolayer. This results in different effective damping factors for the electrons photoemitted by the two sulfur species, which can be compensated by using an attenuation length of 3.30 nm[40] and the estimated thicknesses for the four layers. It was then found that the percentage of bound sulfur atoms increases from 60% for the 0% amino content to almost 90% for the 14% amino percentage (see Table 2). The XPS results clearly showed an increase in the number of PG molecules attached to the surface upon increased amino content in the sample. This suggests that the amino groups also can interact with the gold substrate and promote the self-assembly process, which is in agreement with FT-IRRAS measurements.

Contact angle studies. The balance between the different functional groups located at the interface of a hybrid material strongly affects macroscopic properties like wettability. To analyze the effect of PG-functionalization on the hydrophilic/hydrophobic characteristics of the modified surfaces, water contact angles were measured taking a bare gold surface as reference. The immobilization of the different PG derivatives on the surface caused a marked decrease in the contact angle values (Table 3), reflecting the highly hydrophilic nature imparted by PG and therefore indicating the successful attachment of these polymeric adsorbates on the surface. Note that the PG derivatives comprise a large number of hydrogen-bondable moieties, such as hydroxyl, amino, and ether groups.

A general tendency in the contact angle value of the modified surfaces was to be expected, since the amino content in the adsorbates gradually increases at the expense of the hydroxyl content. Although a trend indicates an increase in the contact angle upon increased amino content, the contact angle of Au/TA–PG–NH_2 6.5% was the lowest, which indicates that this was the most hydrophilic surface of the series. This surprising result suggests that there is a particular balance between the functional groups of this PG derivative that makes this modified surface more hydrophilic than the others. This balance would involve the relation between free, unassociated amino *vs.* associated amino moieties (through Au–amino interactions and/or *via* hydrogen bonding with other PG groups), modifying the hydrogen-donating ability and surface net charge under measurement conditions, and thus determining the surface wettability.

Table 3 Water contact angle results of bare and PG-modified gold surfaces

Contact angle [°] of Au/TA–PG–NH_2, X amino				
Bare Au[a]	0%	6.5%	9%	14%
65	16	<12	20	22

[a] Measured on a precleaned bare gold surface.

Study of the accessibility and availability of the amino groups over the modified surfaces by fluorescence microscopy

PG-modified surfaces represent a good alternative for preparation of specifically functionalized interfaces because the presence of the amino groups can be used, for example, for the covalent binding of biomolecules. Therefore, it is necessary that these amino moieties remain available and accessible for reaction. The first reason for synthesizing PG amino derivatives was to use such amino moieties as attachment points to link biomolecules in a controllable fashion. Since FT-IRRAS and XPS studies pointed out an interaction between the amino groups of the adsorbates with the gold surface, fluorescence studies were performed to assess the real availability and accessibility of $-NH_2$ groups over the surface. For this purpose, labeled probes like proteins or DNA were first bound to the PG-coated surfaces.

Non-specific streptavidin attachment. The attachment of labeled streptavidin to PG-modified surfaces was evaluated (Fig. 5(i)). Strept-Cy3 adsorbs on the substrate by noncovalent interactions. The streptavidin non-specific adsorption increased with the amino content in the sample (Fig. 5(b)). The dependence of the protein attachment with the amino content also demonstrated that these amino moieties remained available and accessible for biomolecule attachment at the interface. This preliminary result also suggests that the PG samples with a low amino content (especially at 6.5%) show a similar resistance to the streptavidin non-specific adsorption than those measured for the PG-derivative without amino groups (0%).

Specific DNA coupling. The specific attachment of DNA to PG derivatized surfaces was carried out by means of the commercial sulfo-SMCC, a heterobifunctional crosslinker in which both succinimidyl-ester and maleimide groups are selective towards amino and sulfhydryl groups, respectively.[45] First, the primary amino groups located on the PG-modified surface rapidly reacted with the *N*-hydroxysuccinimide (NHS) ester moieties of the crosslinker (Fig. 5(ii)), forming an amide bond and leaving active maleimide-pendant groups, which are specific for grafting

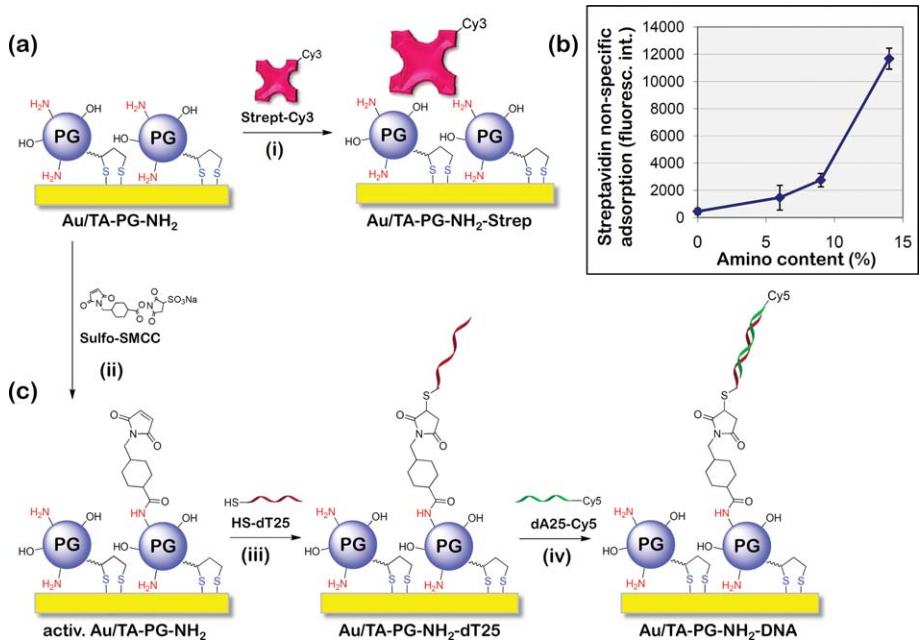

Fig. 5 Schematic representation of fluorescent-probe attachment to PG-modified surfaces, (a and b) non-specific streptavidin attachment and results obtained, and (c) specific DNA coupling.

thiolated biomolecules.[45–47] In a second step, the double bond of the maleimide moiety underwent an alkylation reaction by forming a stable thioether bond with sulfhydryl groups and conjugating a thymine oligonucleotide to the surface (Fig. 5 (iii)).[45,47–49] The hybridization with the dye-marked complementary strand (Fig. 5(iv)) afforded a fluorescent-labeled surface. Fig. 6(a) shows a typical fluorescence micrograph of a gold chip after binding DNA to a modified surface containing amino groups, Au/TA–PG–NH_2 6.5%. Six different fluorescent-DNA spots are present on the chip, demonstrating that the amino moieties on the surface are available and able to react according to the planned sequence. On the contrary, after following the same procedure for the substrate without amino groups (Au/TA–PG–NH_2 0%, Fig. 6(b)), the corresponding picture did not show any fluorescent spots on its surface. This difference is due to the selectivity of succinimidyl-ester towards primary amino groups. Unlike other reactive moieties, succinimidyl esters present a much lower reactivity towards hydroxyl groups than towards primary amino groups. Therefore, the lack of amino groups on the latter substrate leads to negative results, which can be used as a control for the method.

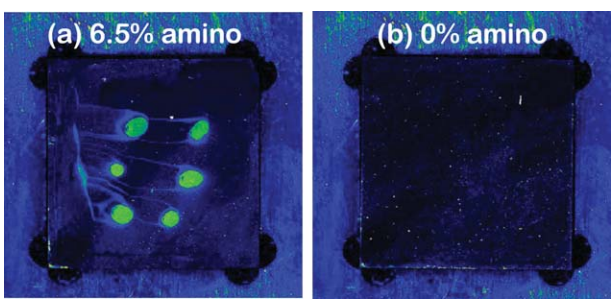

Fig. 6 Typical fluorescence micrographs after binding DNA to PG-coated surfaces with different loading of amino groups: (a) 6.5% (positive) and (b) 0% (negative control).

Evaluation of the protein resistant properties of the functionalized surfaces by SPR

To further study the protein resistant properties of the different PG surfaces in relation to their amino content, SPR studies were conducted. Given its excellent sensitivity (around pg mm^{-2}),[50] this optical surface technique has proven to be a valuable analytical tool for investigating a wide range of biomedically relevant interfaces.[51,52] SPR is advantageous because it can be used to monitor dynamic interactions, such as adsorption–desorption processes in real time and under physiological conditions, and it does not require complex sample preparation or labeling.[51,52]

To test the protein repellant properties of PG samples, four different model proteins were chosen: fibrinogen (340 kDa, pI 5.5), albumin (65 kDa, pI 4.8), lysozyme (14 kDa, pI 11.0), and pepsin (34 kDa, pI 2.0). The choice of these proteins was based on their biological importance and on the different properties (molecular weight and pI) they presented under measurement conditions (PBS, pH 7.4, 10 μL min^{-1} flow rate). Fibrinogen, a large blood plasma glycoprotein that plays a critical role in blood coagulation, is known to adsorb to most material surfaces and is very important in the hemostatic response to implanted materials.[53] Albumin is the most abundant protein in the circulatory system and regulates the colloidal osmotic blood pressure. Lysozyme and pepsin are smaller proteins normally used as complementary highly charged models for electrostatic interactions.[54,55] Note that fibrinogen, albumin, and pepsin are negatively charged, whereas lysozyme and the PG-derivatized surfaces are positively charged under the conducted experimental conditions. Thus, these four proteins were expected to respond

differently to the PG-coated surfaces. Each PG-coated surface was exposed to protein solutions in the flow cell of the SPR spectrometer to determine the amount of adsorbed proteins. The results were expressed relative to a HDT-modified gold surface (see Experimental section), which is known to strongly adsorb proteins by non-specific interactions.[18]

The resistant properties of the PG samples to the four studied proteins depended on the amino content of the PG samples (Fig. 7). An increase in the percentage of amino groups led to a gradual increase in the fibrinogen and pepsin adsorption and to a gradual decrease in the lysozyme adsorption. These results could be interpreted by electrostatic considerations taking into account the net charge of the PG surface and the proteins. As the amino content increased, a more positive charge developed over the surface that enhanced the electrostatic interactions with negatively charged proteins like fibrinogen and pepsin, and repelled positively charged ones like lysozyme.[11] Albumin is also negatively charged under the measurement conditions and, in general terms, an increase of non-specific albumin adsorption with increased amino content was observed.

A global evaluation of the SPR results indicates a general tendency where the protein resistance capability decreases with the increase of the amino content in the coating. Surfaces with amino contents up to 9% still showed very good resistant properties, while the protein resistance rapidly lowered for values higher than 9% except for lysozyme. It needs to be said, however, that the best protein resistant surface was the unfunctionalized PG surface that was as repellent as PEGylated surfaces taken as controls.[18,56]

Remarkably, in all coated surfaces studied here, the protein resistance behavior seems to parallel the tendency observed for the contact angle values, apparently due to a relationship between the higher hydrophilicity of the sample and better protein resistance capability. It has been suggested that surface wettability (generally referred to as hydrophobicity/hydrophilicity) is one of the most important parameters affecting the biological response to an implanted material, including protein adsorption.[57–60] Although the contact angle and non-specific adsorption properties cannot be characterized as collinear, hydrophilicity may be used as a quick way to estimate the material resistance properties.[26] Previous studies have proven by AFM a relationship between higher surface water wettability and lower protein adhesion.[57] In general, water wettability may be a good indicator of the

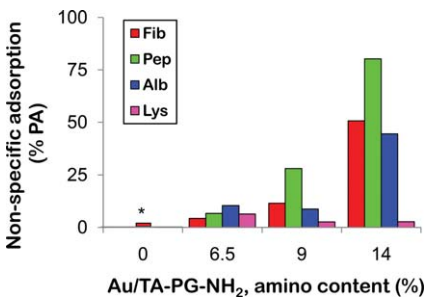

Fig. 7 Non-specific protein adsorption of the different PG-modified surfaces as a function of the amino content. Protein notation: Fib (fibrinogen), Alb (albumin), Pep (pepsin), Lys (lysozyme). Reference: HDT-coated gold surface. * For the other proteins see the previous publication.[22]

propensity of a surface to adsorb proteins, although several other structural features like group dipole moment, hydrogen bonding, and conformational disorder have to be considered.[61] However, the correlation between contact angle values and protein repellency is still controversial. In fact, in a previous study on surfaces coated with PG dendrons, we observed a correspondence between protein resistance and wettability for the –OH terminated series, whereas no relation was observed for the $–OCH_3$ ended series.[22] The same relationship was seen for dendritic[18] and linear[56] –OH terminated PG, probably indicating that this correlation between protein resistance and wettability is characteristic of the –OH ended PG series.

The behavior observed here further supports the idea that protein adsorption cannot be explained in this case only in terms of surface charge or hydrogen-donor ability. In fact, as the amino content increased, a rise in the number of PG anchoring sites with the gold substrate occurred, *i.e.* PG became stickier to the gold surface, as seen by XPS measurements. This effect can distort the conformation of the PG molecules from globular to compressed, flattened structures,[35] as well as restrict the flexibility/chain mobility of the dendritic arms. The latter aspect has proven to reduce the resistance properties of other PG-based coatings.[22] Therefore, we consider that the excellent protein repellent properties evidenced by TA–PG–NH_2 6.5% as well as its higher hydrophilicity is driven by a delicate balance between its functional groups and the substrate, thus determining the hydrogen-donating ability, surface net charge, gold-stickiness, and conformational freedom of the polymers. At the same time, the amino groups of this substrate still remain available to bind biomolecules, as shown by the selective DNA-binding studies.

Conclusions

In summary, we have synthesized dendritic PG derivatives with different numbers of amino groups and have attached them on gold substrates *via* thioctic acid linker. We have demonstrated that the protein resistant properties of the PG-coated surfaces depend on the amino content. Surfaces with amino contents up to 9% still show very good resistant properties. We have also proven the availability of such amino groups for biomolecule attachment as demonstrated by the selective interaction of complementary fluorescently labeled DNA.

The results demonstrate a new way to tailor PG-derivatized surfaces by introducing amino moieties which can act as suitable anchoring sites for specific biomolecule interactions, while maintaining the resistant properties against non-specific protein adhesion. The combination of both characteristics is important in bioelectronics or in the development of biosensing platforms with improved sensitivity.

Acknowledgements

Financial support from Deutscher Akademischer Austausch Dienst (DAAD), Bundesministerium für Bildung und Forschung (BMBF Poly4Bio), the Focus area "Functional Materials at the Nanoscale" (www.nanoscale.fu-berlin.de), SECyT-UNC, FONCyT, and CONICET is acknowledged. The authors thank Alex Krüger and Prof. Wolfgang Kuch for their help with XPS measurements, Andrea Schulz for her technical assistance with

AFM studies, and Dr. Marie Weinhart for helpful discussions. J.I.P. is grateful to CONICET and DAAD for the fellowships granted.

Notes and references

1 M. J. Felipe, P. Dutta, R. Pernites, R. Ponnapati and R. C. Advincula, *Polymer*, 2012, **53**, 427–437.
2 H. Chen, L. Yuan, W. Song, Z. Wu and D. Li, *Prog. Polym. Sci.*, 2008, **33**, 1059–1087.
3 W. Senaratne, L. Andruzzi and C. K. Ober, *Biomacromolecules*, 2005, **6**, 2427–2448.
4 S. Krishnan, C. J. Weinman and C. K. Ober, *J. Mater. Chem.*, 2008, **18**, 3405–3413.
5 T. Mérian and J. M. Goddard, *J. Agric. Food Chem.*, 2012, **60**, 2943–2957.
6 M. Calderón, M. A. Quadir, S. K. Sharma and R. Haag, *Adv. Mater.*, 2010, **22**, 190–218.
7 M. Toda and H. Iwata, *ACS Appl. Mater. Interfaces*, 2010, **2**, 1107–1113.
8 E. Ostuni, R. G. Chapman, R. E. Holmlin, S. Takayama and G. M. Whitesides, *Langmuir*, 2001, **17**, 5605–5620.
9 A. Rastogi, S. Nad, M. Tanaka, N. Da Mota, M. Tague, B. A. Baird, H. D. Abruña and C. K. Ober, *Biomacromolecules*, 2009, **10**, 2750–2758.
10 R. G. Chapman, E. Ostuni, S. Takayama, R. E. Holmlin, L. Yan and G. M. Whitesides, *J. Am. Chem. Soc.*, 2000, **122**, 8303–8304.
11 R. G. Chapman, E. Ostuni, M. N. Liang, G. Meluleni, E. Kim, L. Yan, G. Pier, H. S. Warren and G. M. Whitesides, *Langmuir*, 2001, **17**, 1225–1233.
12 Y. Y. Luk, M. Kato and M. Mrksich, *Langmuir*, 2000, **16**, 9604–9608.
13 E. Österberg, K. Bergström, K. Holmberg, J. A. Riggs, J. M. Van Alstine, T. P. Schuman, N. L. Burns and J. M. Harris, *Colloids Surf., A*, 1993, **77**, 159–169.
14 C. D. Walkey and W. C. W. Chan, *Chem. Soc. Rev.*, 2012, **41**, 2780–2799.
15 S. Zalipsky and J. M. Harris, in *Poly(ethylene glycol)*, American Chemical Society, 1997, pp. 1–13.
16 F. Kawai, T. Kimura, M. Fukaya, Y. Tani, K. Ogata, T. Ueno and H. Fukami, *Appl. Environ. Microbiol.*, 1978, **35**, 679–684.
17 J. Khandare, M. Calderón, N. M. Dagia and R. Haag, *Chem. Soc. Rev.*, 2012, **41**, 2824–2848.
18 C. Siegers, M. Biesalski and R. Haag, *Chem.–Eur. J.*, 2004, **10**, 2831–2838.
19 See http://www.biacore.com/lifesciences/products/Consumables/guide/cm5/index.html.
20 P. Y. J. Yeh, R. K. Kainthan, Y. Zou, M. Chiao and J. N. Kizhakkedathu, *Langmuir*, 2008, **24**, 4907–4916.
21 S. Wang, Y. Zhou, S. Yang and B. Ding, *Colloids Surf., B*, 2008, **67**, 122–126.
22 M. Wyszogrodzka and R. Haag, *Langmuir*, 2009, **25**, 5703–5712.
23 M. Wyszogrodzka and R. Haag, *Biomacromolecules*, 2009, **10**, 1043–1054.
24 G. Gunkel, M. Weinhart, T. Becherer, R. Haag and W. T. S. Huck, *Biomacromolecules*, 2011, **12**, 4169–4172.
25 M. Weinhart, T. Becherer, N. Schnurbusch, K. Schwibbert, H. J. Kunte and R. Haag, *Adv. Eng. Mater.*, 2011, **13**, B501–B510.
26 O. R. Bolduc and J. F. Masson, *Langmuir*, 2008, **24**, 12085–12091.
27 M. Frasconi, C. Tortolini, F. Botre and F. Mazzei, *Anal. Chem.*, 2011, **82**, 7335–7342.
28 Y. Arima and H. Iwata, *J. Mater. Chem.*, 2007, **17**, 4079–4087.
29 T. L. Lasseter, B. H. Clare, N. L. Abbott and R. J. Hamers, *J. Am. Chem. Soc.*, 2004, **126**, 10220–10221.
30 A. Sunder, R. Hanselmann, H. Frey and R. Mülhaupt, *Macromolecules*, 1999, **32**, 4240–4246.
31 S. Roller, H. Zhou and R. Haag, *Mol. Diversity*, 2005, **9**, 305–316.
32 R. G. Chapman, E. Ostuni, L. Yan and G. M. Whitesides, *Langmuir*, 2000, **16**, 6927–6936.
33 T. Gillich, E. M. Benetti, E. Rakhmatullina, R. Konradi, W. Li, A. Zhang, A. D. Schlüter and M. Textor, *J. Am. Chem. Soc.*, 2011, **133**, 10940–10950.
34 H. Frey and R. Haag, *Rev. Mol. Biotechnol.*, 2002, **90**, 257–267.
35 H. Tokuhisa, M. Zhao, L. A. Baker, V. T. Phan, D. L. Dermody, M. E. García, R. F. Pérez, R. M. Crooks and T. M. Mayer, *J. Am. Chem. Soc.*, 1998, **120**, 4492–4501.
36 R. M. Silverstein, F. X. Webster and D. Kiemle, *Spectrometric Identification of Organic Compounds*, John Wiley & Sons, 2005.
37 N. Krasteva, I. Besnard, B. Guse, R. E. Bauer, K. Müllen, A. Yasuda and T. Vossmeyer, *Nano Lett.*, 2002, **2**, 551–555.
38 M. P. Stemmler, Y. Fogel, K. Müllen and M. Kreiter, *Langmuir*, 2009, **25**, 11917–11922.
39 C. D. Wagner, L. E. Davis, M. V. Zeller, J. A. Taylor, R. H. Raymond and L. H. Gale, *Surf. Interface Anal.*, 1981, **3**, 211–225.
40 P. E. Laibinis, C. D. Bain and G. M. Whitesides, *J. Phys. Chem.*, 1991, **95**, 7017–7021.
41 P. J. Cumpson and P. C. Zalm, *Surf. Interface Anal.*, 2000, **29**, 403–406.
42 E. Jagst, Ph.D. thesis, Freie Universität Berlin, Germany, 2010.
43 J. F. Moulder, W. F. Stickle, P. E. Sobol and K. Bomben, in *Handbook of X-ray Photoelectron Spectroscopy*, ed. J. Chastain, Perkin-Elmer Corporation (Physical Electronics), 1992.
44 T. M. Willey, A. L. Vance, C. Bostedt, T. van Buuren, R. W. Meulenberg, L. J. Terminello and C. S. Fadley, *Langmuir*, 2004, **20**, 4939–4944.
45 S. S. Wong, *Chemistry of Protein Conjugation and Cross-Linking*, CRC Press, Inc., Boca Raton, USA, 1993.
46 S.-J. Xiao, S. Brunner and M. Wieland, *J. Phys. Chem. B*, 2004, **108**, 16508–16517.
47 G. MacBeath, A. N. Koehler and S. L. Schreiber, *J. Am. Chem. Soc.*, 1999, **121**, 7967–7968.
48 B. T. Houseman, E. S. Gawalt and M. Mrksich, *Langmuir*, 2002, **19**, 1522–1531.
49 E. A. Smith, M. J. Wanat, Y. Cheng, S. V. P. Barreira, A. G. Frutos and R. M. Corn, *Langmuir*, 2001, **17**, 2502–2507.
50 J. Homola, *Chem. Rev.*, 2008, **108**, 462–493.
51 R. J. Green, R. A. Frazier, K. M. Shakesheff, M. C. Davies, C. J. Roberts and S. J. B. Tendler, *Biomaterials*, 2000, **21**, 1823–1835.
52 Y. Arima, M. Toda and H. Iwata, *Adv. Drug Delivery Rev.*, 2011, **63**, 988–999.
53 P. Soman and C. A. Siedlecki, *Langmuir*, 2011, **27**, 10814–10819.
54 T. Ekblad, O. Andersson, F.-I. Tai, T. Ederth and B. Liedberg, *Langmuir*, 2009, **25**, 3755–3762.
55 Y. Xu, M. Takai and K. Ishihara, *Biomacromolecules*, 2009, **10**, 267–274.
56 M. Weinhart, I. Grunwald, M. Wyszogrodzka, L. Gaetjen, A. Hartwig and R. Haag, *Chem.–Asian J.*, 2010, **5**, 1992–2000.
57 L. C. Xu and C. A. Siedlecki, *Biomaterials*, 2007, **28**, 3273–3283.
58 S. Herrwerth, W. Eck, S. Reinhardt and M. Grunze, *J. Am. Chem. Soc.*, 2003, **125**, 9359–9366.
59 A. Rosenhahn, S. Schilp, H. J. Kreuzer and M. Grunze, *Phys. Chem. Chem. Phys.*, 2010, **12**, 4275–4286.
60 J. M. Berg, L. G. T. Eriksson, P. M. Claesson and K. G. N. Borve, *Langmuir*, 1994, **10**, 1225–1234.
61 G. B. Sigal, M. Mrksich and G. M. Whitesides, *J. Am. Chem. Soc.*, 1998, **120**, 3464–3473.